

Natural convection in a nanofluid filled prismatic cavity with non-isothermal bottom wall

Salma Parvin ^{1*}, Rehena Nasrin ¹ and Raju Chowdhury ^{1,2}

¹ Department of Mathematics, Bangladesh University of Engineering & Technology, Dhaka-1000, Bangladesh,

² Department of Natural Science, Stamford University Bangladesh, Dhaka-1209, Bangladesh.

*E-mail: salpar@math.buet.ac.bd

Abstract

The present paper executes the natural convection flow and heat transfer inside a prismatic enclosure with non-uniform temperature distribution maintained at the bottom wall. The water-Al₂O₃ nanofluid is used as the heat transfer medium through the enclosure. Finite Element Method of Galerkin's weighted residual scheme is used to solve the transport equations with appropriate boundary conditions. Computations are done for various Rayleigh number Ra (10^3 to 10^6) for nanofluid as well as for the base fluid. Isotherms, streamlines and heat lines, local and average heat transfer are presented graphically. Results show that nanofluid gives the higher transfer rate than that of the base fluid for all the considered Ra values.

Keywords: Natural convection; finite element method; heatline, nanofluid; prismatic enclosure; non isothermal wall.

1. Introduction

Natural convection in enclosures finds its applications in geophysics, geothermal reservoirs, insulation of building, heat exchanger design, building structure etc. that motivates many researchers to perform numerical simulation to investigate the flow pattern, temperature distribution, and heat flow. The low thermal conductivity of conventional heat transfer fluids, commonly water, has restricted designers. Fluids containing nanosized solid particles offer a possible solution to conquest this problem. Most of the available literature on this topic concerns regular geometries such as rectangular or square enclosures, while actual applications demand the consideration of irregular shapes. Literature reviews on natural convection inside triangular, trapezoidal and rhombic enclosures are available in [1-5].

The heat recovery system or true path of convective heat transfer can be visualized by 'heatline' method. Heatlines represent heatflux lines which represent the trajectory of heat flow in the system and they are normal to the isotherms for conductive heat transfer. Kimura and Bejan [6] and Bejan [7] first introduced the concept of heatline. Various applications using heatlines were studied in [8-14]. Dalal and Das [15] have used heatline method for the visualization of flow in a complicated cavity. Recently, Yaseen [16] has studied and analyzed numerically the steady natural convection flow in a prismatic enclosure with strip heater on bottom wall. Recently Ahmed et.al [17] performed numerical analysis for natural convection flows within prismatic enclosures based on heatline approach.

Heat transfer in cavities filled with nanofluid is the research interest of many researchers. Parvin et al. [18] studied the natural convection heat transfer in an enclosure with a heated body filled with nanofluid. Nasrin and Parvin [19] investigated numerically the buoyancy-driven flow and heat transfer in a trapezoidal cavity filled with water-Cu nanofluid. In their work, a correlation is developed graphically for the average Nusselt number as a function of the Prandtl number as well as the cavity aspect ratio. Abu- Nada and Chamkha [20] performed a numerical study of natural convection heat transfer in a differentially heated enclosure filled with CuO-EG-Water nanofluid. Heat Transfer and Entropy Generation in an Odd-shaped Cavity filled with Nanofluid is analyzed by Parvin and Chamkha [21]. It must be noticed that, adding nanoparticles into the base fluid does not always increase its thermal conductivity [22]. Parvin et al. [23] numerically investigated the natural convection heat transfer from a heated cylinder contained in a square enclosure filled with water-Cu nanofluid. Their results indicated that heat transfer augmentation is possible using highly viscous nanofluid.

The above literature contains many investigations into the heat transfer performance of natural convection of nanofluid in regular shaped cavities. However, a comprehensive analysis on heat flow during natural convection cooling by nanofluid in irregular enclosure with the heatline approach is yet to appear in the literature. Accordingly, the present study performs a numerical investigation into the natural convection heat flow within a prism shaped cavity containing nanofluid with non isothermal bottom wall. The study focuses specifically on the effects of the free convective parameter on the streamlines, isotherm distribution, heatlines and average Nusselt number for nanofluid as well as water.

2. Governing Equations

The physical domain is shown in Fig. 1. Under the Boussinesq approximation, the governing equations for steady two dimensional laminar incompressible flows in dimensionless form are:

$$\frac{\partial U}{\partial X} + \frac{\partial V}{\partial Y} = 0 \quad (1)$$

$$U \frac{\partial U}{\partial X} + V \frac{\partial U}{\partial Y} = -\frac{\rho_f}{\rho_{nf}} \frac{\partial P}{\partial X} + Pr \frac{\nu_{nf}}{\nu_f} \left(\frac{\partial^2 U}{\partial X^2} + \frac{\partial^2 U}{\partial Y^2} \right) \quad (2)$$

$$U \frac{\partial V}{\partial X} + V \frac{\partial V}{\partial Y} = -\frac{\rho_f}{\rho_{nf}} \frac{\partial P}{\partial Y} + Pr \frac{\nu_{nf}}{\nu_f} \left(\frac{\partial^2 V}{\partial X^2} + \frac{\partial^2 V}{\partial Y^2} \right) + Ra Pr \frac{(1-\chi)\rho_f\beta_f + \chi\rho_s\beta_s}{\rho_{nf}\beta_f} \theta \quad (3)$$

$$U \frac{\partial \theta}{\partial X} + V \frac{\partial \theta}{\partial Y} = \frac{\alpha_{nf}}{\alpha_f} \left(\frac{\partial^2 \theta}{\partial X^2} + \frac{\partial^2 \theta}{\partial Y^2} \right) \quad (4)$$

where, $\rho_{nf} = (1-\chi)\rho_f + \chi\rho_s$ is the density, $(\rho C_p)_{nf} = (1-\chi)(\rho C_p)_f + \chi(\rho C_p)_s$ is the heat capacitance, $\beta_{nf} = (1-\chi)\beta_f + \chi\beta_s$ is the thermal expansion coefficient, $\alpha_{nf} = k_{nf}/(\rho C_p)_{nf}$ is the thermal diffusivity, $\mu_{nf} = \mu_f(1-\chi)^{-2.5}$ is dynamic viscosity and $k_{nf} = k_f \frac{k_s + 2k_f - 2\chi(k_f - k_s)}{k_s + 2k_f + \chi(k_f - k_s)}$ is the thermal conductivity of the

nanofluid and $X = \frac{x}{L}$, $Y = \frac{y}{L}$, $U = \frac{uL}{\alpha}$, $V = \frac{vL}{\alpha}$, $\theta = \frac{T - T_c}{T_h - T_c}$, $P = \frac{pL^2}{\rho\alpha^2}$, $Pr = \frac{\nu}{\alpha}$, $Ra = \frac{g\beta(T_h - T_c)L^3 Pr}{\nu^2}$

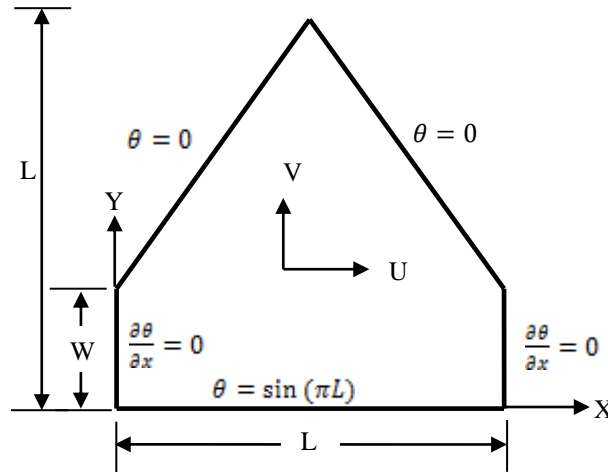


Fig.1: Schematic diagram of the physical system

The boundary conditions can be summarized by the following equations:

- At the bottom wall: $U = 0, V = 0, \theta = \sin(\pi L)$
- For the side walls: $U = 0, V = 0, \frac{\partial \theta}{\partial X} = 0$
- For the inclined walls: $U = 0, V = 0, \theta = 0$

The relationships between streamfunction ψ and velocity components U, V for two-dimensional flows are

$$U = \frac{\partial \psi}{\partial Y} \text{ and } V = -\frac{\partial \psi}{\partial X} \quad \text{which give a single equation } \frac{\partial^2 \psi}{\partial X^2} + \frac{\partial^2 \psi}{\partial Y^2} = \frac{\partial U}{\partial Y} - \frac{\partial V}{\partial X} \quad (5)$$

The no-slip condition is valid at all boundaries as there is no cross-flow. Hence $\psi = 0$ is used for boundaries. The heat flow within the enclosure is displayed using the heatfunction Π obtained from conductive heat fluxes $\left(-\frac{\partial \theta}{\partial X}, -\frac{\partial \theta}{\partial Y}\right)$ as well as convective heat fluxes $(U\theta, V\theta)$. The heatfunction satisfies the steady energy balance

equation such that $\frac{\partial \Pi}{\partial Y} = U\theta - \frac{\partial \theta}{\partial X}$ and $-\frac{\partial \Pi}{\partial X} = V\theta - \frac{\partial \theta}{\partial Y}$ which yield a single equation

$$\frac{\partial^2 \Pi}{\partial X^2} + \frac{\partial^2 \Pi}{\partial Y^2} = \frac{\partial}{\partial Y}(U\theta) - \frac{\partial}{\partial X}(V\theta) \quad (6)$$

The local and average Nusselt number may be expressed as $Nu_{local} = -\left(\frac{k_{nf}}{k_f}\right) \frac{\partial \theta}{\partial N}$ and

$$Nu = -\frac{1}{S} \int_0^S \left(\frac{k_{nf}}{k_f}\right) \frac{\partial \theta}{\partial N} dN \quad \text{where } S \text{ is the non-dimensional length of the surface.}$$

3. Numerical Method

The numerical procedure used in this study is based on the Galerkin weighted residual method of finite element. The solution domain is discretized into finite element meshes, which are composed of non-uniform triangular elements. Then the nonlinear governing partial differential equations are transferred into a system of integral equations by applying Galerkin weighted residual method. The integration involved in each term of these equations is performed by using Gauss's quadrature method. The nonlinear algebraic equations so obtained are modified by imposition of boundary conditions. These modified nonlinear equations are transferred into linear algebraic equations by using Newton's method. Finally, these linear equations are solved by using Triangular Factorization method. The convergence criterion set to be $|\psi^{n+1} - \psi^n| \leq 10^{-4}$, where n is the number of iteration and ψ is a function U, V and θ .

3.1 Grid Independent Test

An extensive mesh testing procedure is conducted to guarantee a grid-independent solution for $Ra = 10^5$ and $Pr = 6.2$, $\chi = 0$ in a prismatic enclosure. Five different non-uniform grid systems with the following number of elements within the resolution field: 454, 926, 1504, 2270 and 9948 are examined. The numerical scheme is carried out for highly precise key in the average Nusselt (Nu) number to understand the grid fineness as shown in Fig. 2. The scale of the average Nusselt numbers for 2270 elements shows a little difference with the results obtained for the other elements. Hence, considering the non-uniform grid system of 2270 elements is preferred for the computation.

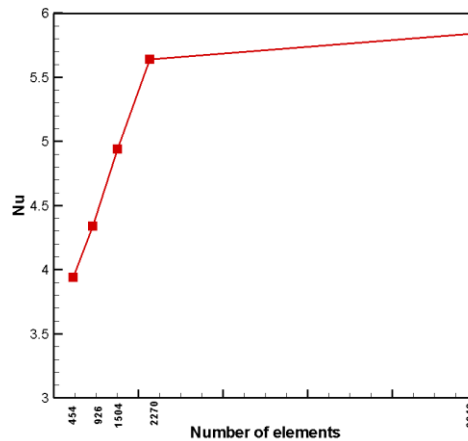


Fig. 2 Grid independent test

4. Result and Discussion

The numerical computation has been carried out through the finite element method to analyze natural convection within a nanofluid filled prismatic enclosure based on heatline concept. Results of isotherms, streamlines and heatlines for various values of Rayleigh number Ra ($= 10^3$ to 10^6) with Prandtl number $Pr = 6.2$ for both nanofluid and base fluid in the prismatic enclosure are displayed. The Al_2O_3 nanoparticle volume fraction χ is chosen as 5%. In addition, the values of local and average Nusselt number at the bottom have been calculated for the mentioned parameter.

4.1 Effect on Isotherms

The influence of Rayleigh number Ra on isotherms for the present configuration has been demonstrated in Fig. 3(a). The pattern of isotherms is smooth for low Ra and is symmetric to the central vertical line for all the considered values of Ra . At higher Rayleigh number, a thermal plume rises from the middle of the bottom wall because of sinusoidal boundary temperature. The isothermal lines for pure water are more distorted than that of nanofluid.

4.2 Effect on Streamlines

Streamlines corresponding to different Rayleigh number Ra are shown in Fig. 3(b). It is seen from the figure that the trend of streamlines are similar for all cases. There are two symmetric circulation cells formed inside the enclosure. With the increasing value of the Ra , the streamlines are less dense near the central vertical line. It is noteworthy to mention that the central cores of the circulatory cells increase in size for higher values of Ra indicate the greater strength of the flow. Higher flow intensity is seen for the base fluid in comparison to the nanofluid.

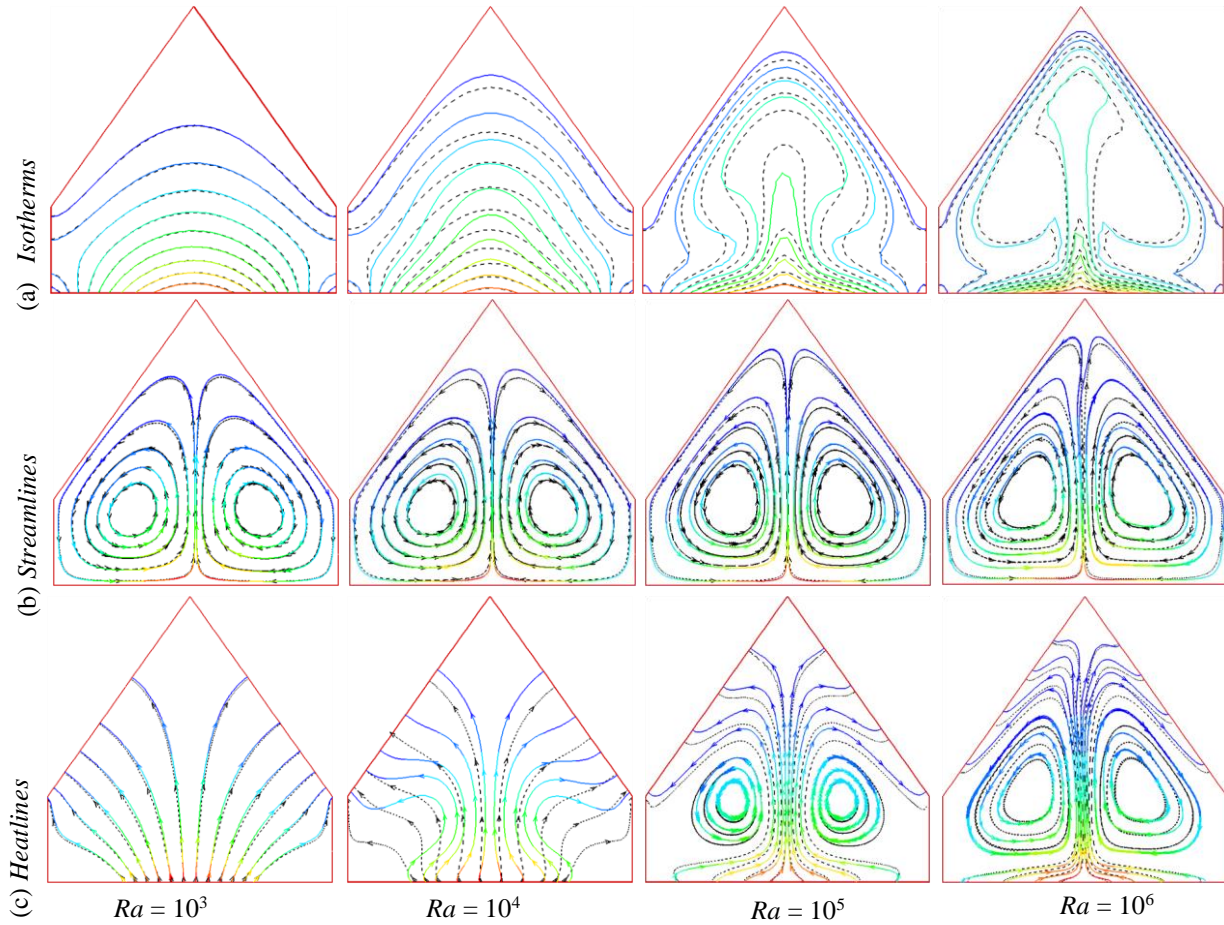


Fig. 3. Effect of Rayleigh number Ra on (a) isotherms (b) streamlines and (c) heatlines for base fluid (solid colored lines) and nanofluid (dashed black lines)

4.3 Effect on Heatlines

The heatlines are constructed based on the thermal boundary conditions. As seen from the Fig. 3(c), the heatlines are similar to streamlines at the core signifying convective heat flow and a large amount of heat flow occurs from the middle portion of the bottom wall as seen from dense heatlines. The two heat circulations in the system are observed and a very intense heat flow occurs across the middle of the cavity represented by dense heatline for large Rayleigh number. It is interesting to observe that heat transport in a large regime at the core is due to strong natural convection. The large regime of convection is due to the large amount of heat transport from the bottom wall associated with large intensity of circulations. At $Ra = 10^3$, heat transfer occur mainly by conduction where, heatlines are perpendicular to the isotherms. Laminar patterns of heatlines are slightly disturbed for $Ra = 10^6$.

4.4 Local and Average Nusselt number

Fig. 4(a)-(c) shows the distribution of the local and average Nusselt number of the bottom wall versus the Rayleigh number Ra for nanofluid and water. Fig 4(a) and 4(b) present the local heat transfer rate for base fluid and nanofluid respectively. General observation is that the Nusselt number increases sharply for dominant natural convection region ($Ra > 10^4$) for both the fluids. Similar trend of local and average heat transfer rate is seen for both the fluid where as nanofluid shows the higher heat transfer rate. That is adding nanoparticles increases the thermal conductivity which leads to enhanced heat transfer.

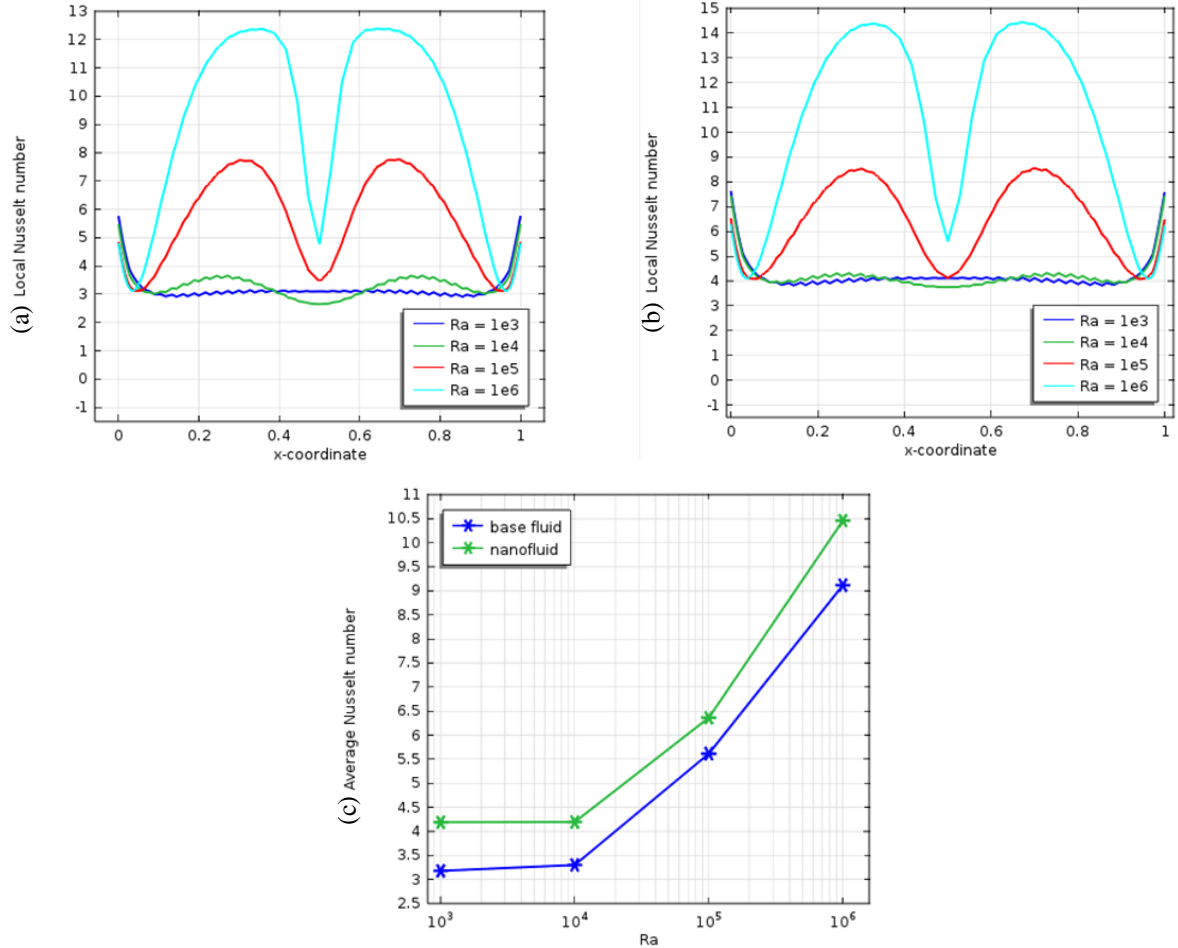


Fig. 4. Effect of Rayleigh number Ra on (a) local Nusselt number for base fluid (b) local Nusselt number for nanofluid and (c) average Nusselt number

5. Conclusion

The current investigation performed a physical as well as computational insight due to heatflow for natural convection within a prismatic enclosure filled with nanofluid. The major conclusions are the following:

- Isotherms, streamlines and heatlines are found to be smooth and the heatlines are seen normal to the isotherm during the lower convection regime.
- For higher Rayleigh number, heat transfer and flow strength increases and heatlines take the flow pattern.
- for nanofluid, heat transfer becomes higher than that of base fluid.

6. Acknowledgement

The present work is done in the department of mathematics BUET.

7. References

- [1] T. Basak, G. Arvind and S. Roy, Visualization of heat flow due to natural convection within triangular cavities using Bejan's heatline concept, *Int. J. Heat Mass Transfer*, vol. 52 (11-12), pp. 2824-2833, 2009.
- [2] T. Basak, S. Roy, D. Ramakrishna and I. Pop, Visualization of Heat Transport during Natural Convection Within Porous Triangular Cavities via Heatline Approach, *Numerical Heat Transfer, Part A*, vol. 57 (6), pp. 431-452, 2010.
- [3] T. Basak, S. Roy and I. Pop, Heat flow analysis for natural convection within trapezoidal enclosures based on heatline

concept, *Int. J. Heat Mass Transfer*, vol. 52 (11-12), pp. 2471–2483, 2009.

- [4] R. Anandalakshmi and T. Basak, Heatline based thermal management for natural convection in porous rhombic enclosures with isothermal hot side or bottom wall, *Energy Conversion and Management*, vol. 67, pp. 287–296, 2013.
- [5] T. Basak, S. Roy and I. Pop, Heat flow analysis for natural convection within trapezoidal enclosures based on heatline concept, *Int. J. Heat Mass Transfer*, vol. 52, pp. 2471–2483, 2009.
- [6] S. Kimura and A. Bejan, The heatline visualization of convective heat-transfer, *ASME J. Heat Transfer*, vol. 105 (4), pp. 916–919, 1983.
- [7] Bejan, Convection Heat Transfer, third ed., Wiley, Hoboken, NJU, 1984.
- [8] F.L. Bello-Ochende, A heat function formulation for thermal convection in a square cavity, *Int. Commun. Heat Mass Transfer*, vol. 15, pp. 193–202, 1988.
- [9] V.A.F. Costa, Heatline and massline visualization of laminar natural convection boundary layers near a vertical wall, *Int. J. Heat Mass Transfer*, vol. 43 (20), pp. 3765–3774, 2000.
- [10] V.A.F. Costa, Unified streamline, heatline and massline methods for the visualization of two-dimensional heat and mass transfer in anisotropic media, *Int. J. Heat Mass Transfer*, vol. 46 (8), pp. 1309–1320, 2003.
- [11] V.A.F. Costa, Bejan’s heatlines and masslines for convection visualization and analysis, *Appl. Mech. Rev.*, vol. 59 (3), pp. 126–145, 2006.
- [12] Mukhopadhyay, X. Qin, S.K. Aggarwal and I.K. Puri, On extension of heatline and massline concepts to reacting flows through use of conserved scalars, *ASME J. Heat Transfer*, vol. 124 (4), pp. 791–799, 2002.
- [13] Mukhopadhyay, X. Qin, S.K. Aggarwal and I.K. Puri, Visualization of scalar transport in non-reacting and reacting jets through a unified “heatline” and “massline” formulation, *Numer. Heat Transfer, Part A*, vol. 44 (7), pp. 683–704, 2003.
- [14] Q.H. Deng and G.F. Tang, Numerical visualization of mass and heat transport for conjugate natural convection/heat conduction by streamline and heatline, *Int. J. Heat Mass Transfer*, vol. 45 (11), pp. 2373–2385, 2002.
- [15] Dalal and M.K. Das, Heatline method for the visualization of natural convection in a complicated cavity, *Int. J. Heat Mass Transfer*, vol. 51 (1-2), pp. 263–272, 2008.
- [16] S. J. Yaseen, Numerical study of steady natural convection flow in a prismatic enclosure with strip heater on bottom wall using FLEXPDE, *Diyala Journal of Engineering Sciences*, vol. 7 (1), pp. 61–80, 2014.
- [17] K. F. U. Ahmed, S. Parvin and Ali J. Chamkha, Numerical analysis based on heatline approach for natural convection flows within prismatic enclosures, *Int. J. Energy & Technology* Vol. 7 (2), pp. 19–29, 2015
- [18] S. Parvin, K.F.U. Ahmed, M.A. Alim and N.F. Hossain, Heat transfer enhancement by nanofluid in a cavity containing a heated obstacle, *Int. J. Mechanical and Materials Eng.(IJMME)*, 7 (2) pp. 128–135, 2012.
- [19] Rehana Nasrin, Salma Parvin, Investigation of buoyancy-driven flow and heat transfer in a trapezoidal cavity filled with water–Cu nanofluid, *Int. Commun. Heat Mass Transfer* 39 (1) pp. 270–274, 2012.
- [20] E. Abu-Nada and A. J. Chamkha, Effect of nanofluid variable properties on natural convection in enclosures filled with a CuO-EG-Water nanofluid, *Int. J. Therm. Sci.* 49 pp. 2339–2352, 2010.
- [21] Salma Parvin and A.J. Chamkha, An Analysis on Free Convection Flow, Heat Transfer and Entropy Generation in an Odd-shaped Cavity filled with Nanofluid, *Int. Commun. Heat Mass Transfer* 54 pp. 8–17, 2014.
- [22] S. Teja, M. P. Beck, Y. Yuan and P. Warrier, The limiting behavior of the thermal conductivity of nanoparticles and nanofluids, *J. Applied Physics*, 107 pp. 114319, 2010.
- [23] Salma Parvin, M.A. Alim, N.F. Hossain, Prandtl number effect on cooling performance of a heated cylinder in an enclosure filled with nanofluid, *Int. Commun. Heat Mass Transfer*. 39, pp. 1220–1225, 2012.

Nomenclature

C_p	specific heat [$\text{J kg}^{-1} \text{K}^{-1}$]	U, V	dimensionless velocity components
g	acceleration due to gravity [ms^{-2}]	x, y	distance along x - and y - coordinates
k	thermal conductivity [$\text{W m}^{-1} \text{K}^{-1}$]	X, Y	dimensionless distance along x - and y - coordinates
L	length of the base and height [m]		Greek symbols
Nu	Nusselt number	α	thermal diffusivity [ms^{-2}]
p	dimensional pressure [Pa]	ν	kinematic viscosity of the fluid [$\text{m}^2 \text{s}^{-1}$]
P	dimensionless pressure	θ	dimensionless temperature
Pr	Prandtl number	χ	nanoparticle volume fraction
Ra	Rayleigh number	ρ	density [kg m^{-3}]
T	temperature [K]	ψ	Stream function
u, v	velocity components [ms^{-1}]	Π	heatfunction